Available online at www.sciencedirect.com
SCIENCE DIRECT®
Computers & Fluids 33 (2004) 521–531
computers & fluids
www.elsevier.com/locate/compfluid

Transverse momentum micromixer optimization with evolution strategies

Sibylle D. Müller [a,*], Igor Mezić [b], Jens H. Walther [a], Petros Koumoutsakos [a,c]

[a] *Institute of Computational Science, Swiss Federal Institute of Technology (ETH), 8092 Zürich, Switzerland*
[b] *Department of Mechanical and Environmental Engineering, University of California, Santa Barbara, CA 93106-5070, USA*
[c] *NASA Ames Research Center, Mail Stop 202A-1, Moffett Field, CA 94035, USA*

Received 28 October 2002; received in revised form 3 July 2003; accepted 3 July 2003

Abstract

We conduct a numerical study of mixing in a transverse momentum micromixer. Good values for actuation frequencies can be determined using simple kinematic arguments, and evolution strategies are introduced for the optimization of mixing by adjusting the control parameters in micromixer devices. It is shown that the chosen optimization algorithm can identify, in an automated fashion, effective actuation parameters. We find that optimal frequencies for increasing number of transverse channels are superposable despite the non-linear nature of the mixing process.

1. Introduction

The use of integrated microelectromechanical systems (MEMS) is expanding rapidly due to improvements in microfabrication technology. MEMS have applications in a variety of industries, including the automotive, aerospace, computer, and biomedical industries. Micrototal analysis systems (mTAS) are being developed for drug discovery, drug delivery, and chemical sensing [5]. The performance of these devices can be limited by the rate in which mixing occurs at the microscale. Mixing of two fluids can be enhanced when the interface between the fluids is increased through stretching and folding, so that diffusion between the fluids occurs only over a relatively

* Corresponding author. Tel.: +41-1-632-6827; fax: +41-1-632-1703.
E-mail address: muellers@inf.ethz.ch (S.D. Müller).

0045-7930/$ - see front matter © 2003 Elsevier Ltd. All rights reserved.
doi:10.1016/j.compfluid.2003.07.004

small distance [15]. In microdevices, fluids are often mixed through pure molecular diffusion. However, depending upon the rate at which diffusion occurs, the diffusion time scale may be too large. Microscale mixers can be divided into passive and active mixers.

Passive mixers have been developed in [3,4]. Miyake et al. [14] designed a mixer using an array of 400 micronozzles. Each nozzle produced a plume of fluid, which increased the interface area between the two fluids. Liu et al. [13] developed a passive three-dimensional serpentine microchannel to enhance mixing by chaotic advection. Their three-dimensional mixer shows promise for passive mixing at Reynolds numbers ranging from 6 to 70. More recently, a three-dimensional serpentine mixer has been investigated by Yi and Bau [21].

Most of the active mixing strategies are based upon the principle of chaotic advection [2,15]. Chaotic advection can be used to control the rate and quality of mixing [6]. Evans et al. [7] developed a planar microfabricated mixer that uses a source–sink system to induce chaotic advection. Here, unmixed fluid is pumped into a mixing chamber, and then two source–sink systems are alternately pulsed to mix the fluid.

Despite these efforts, the problem of mixing at the microscale remains. Many of the mixing strategies are effective, but only at specific flow regimes. Here, we present optimization of an active micromixer, described in [18,19] that can be adapted to achieve effective mixing over various flow conditions. The working principle of the mixer is to perturb the motion of two fluid streams flowing through a main channel by oscillating flow emanating from three pairs of secondary channels at specified frequencies and phase shifts (see Fig. 2). We call the device transverse momentum micromixer (TMM). A related mixer design that incorporates three staggered secondary channels has recently been proposed by Lee et al. [11].

In order to pursue optimization of the parameters of the TMM, we employ stochastic, non-gradient based algorithms, namely evolution strategies (ES). Non-gradient based algorithms such as ES are an interesting alternative to gradient based optimization methods as they are able to circumvent difficulties encountered in the latter. Evolution strategies are highly parallel algorithms, capable of optimizing noisy, multi-modal, and discontinuous functions. Usually, they do not exhibit the high convergence rate of gradient based methods but their cost is compensated by the highly parallel character of the method.

In Section 2, we describe the micromixing device and analyze mixing in this device. Section 3 describes evolution strategies and in particular the covariance matrix adaptation used in the optimization of the micromixer. Section 4 reports and discusses the results of the optimization, followed by conclusions in Section 5.

2. Micromixer device and theory of mixing analysis

2.1. Micromixing design

The proposed mixer is actuated to enhance mixing in a straight channel. Flow in the main channel is manipulated by controlling time-dependent flow from six secondary channels. From these secondary channels, time-dependent cross-flow momentum is imparted on the main channel flow which alters the trajectories of the fluid elements. Physically, in experiments performed at the University of California, Santa Barbara, plungers are introduced into side channels, one at each

side of the side-channel pair. The plungers in the side-channel pair are operated out-of-phase. As seen from Fig. 2, the main channel is $2h$ in height and $13.5h$ in length where h is a varying length scale and $h = 100$ μm for the experimental setup. Secondary channels are $h/2$ in width and $5h$ in length. The inlet velocity $U(y)$ of the main channel is assumed parabolic,

$$U(y, x = 0) = U_m\left(1 - \left(\frac{y}{h}\right)^2\right), \quad |y| \leqslant h. \tag{1}$$

The plug flow in each secondary channel pair is characterized by a sinusoidal velocity

$$V_i = \widehat{V}_i \sin(2\pi f_i t + \phi_i), \quad i \in 1, 2, 3, \tag{2}$$

where f_i is the oscillation frequency, ϕ_i the phase shift relative to the first pair of secondary channels, and $\widehat{V}_i$ the velocity amplitude. We study mixing in a scaled mixer with $U_m = 1$ m/s and $h = 1$ m. In the following, the SI-units are omitted. The viscosity of the flow is $\nu = 0.4$, and hence the Reynolds number $Re = U_m 2h/\nu = 5$. Within this work, we set $\widehat{V}_1 = \widehat{V}_2 = \widehat{V}_3 = 2U_m = 2$ and $\phi_2 = \pi$, $\phi_3 = 0$ as in Volpert et al. [19].

The physical nature of the flow in the TMM can be described in terms of combined action of horizontal and vertical shear flow profiles. A fluid particle introduced at the entrance of the TMM travels predominantly horizontally until it reaches the region of intersection with the first transverse channel. Here, vertical momentum is imparted onto the particle resulting in a vertical motion of the initially horizontal fluid layer. After the exit from the zone of intersection with the first transverse channel, the particle moves horizontally due to the approximate parabolic velocity profile. The process is repeated upon encounter with the second transverse channel. The unsteady flow in the secondary channels is essential for the mixing process. In the present study, we shall assume a periodically varying flow in the secondary channels (Eq. (2)) and inquire the optimal frequencies f_i of the actuation.

When the fluid particle is in the zone before or after the transverse channels or between two side channels, its motion can be approximated with reasonable accuracy as induced by the parabolic velocity profile (Eq. (1)) by

$$\dot{x} = U_m\left(1 - \left(\frac{y}{h}\right)^2\right). \tag{3}$$

Thus, the particle moves only horizontally, but adjacent layers of fluid particles experience differential motion (shear). In the zone where transverse channels and main channel intersect, the motion can be approximated as a combination of the vertical, time-dependent oscillating profile, see Eq. (2), by

$$\dot{y} = \widehat{V}_i \sin(2\pi f_i t + \phi_i)\left(1 - \left(\frac{4(x - x_{mi})}{h}\right)^2\right), \tag{4}$$

where x_{mi} is the distance from the entrance to the device to the middle of the ith transverse channel. In order to effectively use the shear, the vertical motion must reorient horizontal fluid elements to a vertical position, effectively applying a "Baker's transformation" [20] to the fluid. We estimate the conditions for optimal mixing by asking that a fluid particle at the lower wall of

the main channel is displaced to the upper wall during one actuation period, thus $l = 4h$ for the distance the particle has travelled during one period.

2.2. Theory of mixing

To estimate the optimal frequency for the first side-channel pair, let in a first approximation $V^* = 2U_m$ be the maximum velocity in the side channel. This yields a frequency of $f = \frac{1}{2}$, used as a start point for evolutionary optimization described later. In a second approximation, we compute from the spatial average velocity $\frac{2}{3}V^*$ the frequency $f = \frac{1}{3}$. In a third approximation, the temporal average velocity is $\frac{4}{3\pi}V^*$, yielding a frequency of $f = \frac{4V^*}{3\pi l} = \frac{2}{3\pi} \approx 0.21$. With enhanced approximations, the frequency decreases.

For a mixer with three side channels, we need to study the ratio between the three frequencies. Note that in the process of reorienting horizontal slabs into vertical ones we half the average length of the fluid element. If we applied the same frequency again in the second channel, not much would be achieved in terms of mixing. The optimal frequency for the second transverse channel, by the same reasoning as for the first channel, must be approximately twice the frequency in the first channel. By similar arguments, the length of the fluid element becomes 1/4 of the original one after the second transverse channel. Continuing this logic, after the third channel we obtain 1/8 of the original length scale with four times the frequency of the first channel. Note that these consideration yield different numbers than the series of "rational" frequencies $\left(\frac{1}{2}, \frac{1}{3}, \frac{1}{4}\right)$, and "irrational" frequencies $\left(\frac{1}{2\sqrt{5}}, \frac{1}{2\sqrt{2}}, \frac{1}{2}\right)$ as proposed in [19]. The reason is that the frequency in the side channel proposed in [19] was based on the maximum velocity in the side channel, rather than the average, and that the second and third frequencies were based on breaking key bends of rational and irrational frequency motion in the flow, in the spirit of "twist map" theory [12].

3. Evolution strategies

3.1. Why evolution strategies?

Evolution strategies are stochastic optimization algorithms which address the following search problem: Minimize an objective function which is a mapping from a real-valued parameter vector $\boldsymbol{x} \in \mathscr{R}^n$ to $\mathscr{R}$ where n is the number of optimization parameters. They are based on biologically inspired mechanisms such as reproduction, mutation, recombination, and selection applied on individuals in a population. The members of a population are capable of evolving by adapting to their environment.

In contrast to many deterministic algorithms, evolution strategies require only the value of the objective function for a given point in the parameter space, but do not rely on gradient or curvature information like gradient or Newton methods. This is an advantage for many practical problems such as the micromixing optimization for which the analytical gradient is not available and an approximation of the gradient is rather difficult or even impossible due to noise in measuring the objective function. Certain evolution strategies obtain gradient or curvature information in the course of the optimization without losing their robustness in noisy environments.

On the other hand, non-gradient based algorithms do not possess highly efficient convergence like, e.g., the conjugate gradient method, but this disadvantage is compensated by the important feature of evolutionary algorithms being inherently parallel. Among non-gradient methods, the choice of stochastic evolution strategies instead of a deterministic algorithm is motivated by the expected noise in the objective function, resulting from the numerical flow calculations.

3.2. A basic evolution strategy and adaptation

The $(1+1)$ evolution strategy is the simplest evolution scheme and was developed by Rechenberg and Schwefel in 1963, initially to optimize experimental fluid dynamics problems [16]. This strategy consists of two individuals, one parent and one child. Each individual is identified by a parameter vector $\boldsymbol{x}$ with n components, which undergoes *mutation* and *selection*. In the mutation step, the strategy generates a child $\boldsymbol{x}_c^{(g)}$ at generation g, by adding a normally distributed random vector $\boldsymbol{z}^{(g)}$ to the parent vector $\boldsymbol{x}_p^{(g)}$, $\boldsymbol{x}_c^{(g)} = \boldsymbol{x}_p^{(g)} + \boldsymbol{z}^{(g)}$. In the selection step, the objective function value for both parent and child is calculated. For minimization, the one with the smaller function value is then chosen to be the parent vector of the next generation.

Generalizations of the $(1+1)$ evolution scheme operate on larger populations with $\mu \geqslant 1$ parents and $\lambda > \mu$ children.

One of the main features of evolution strategies is the adaptation of one or more mutation parameter(s). These parameters characterize the mutation distribution [17]. The adaptation of the mutation distribution is regarded to be a crucial factor in the convergence rate as well as the global search properties of an evolution strategy. In Fig. 1, three mechanisms for adaptation of global and individual step sizes (standard deviations of the normal distribution) are illustrated for a two-dimensional function. The figure shows lines of equal probability to place children where the center of the circles and ellipses is the location of the parent individual. What can be adapted? We distinguish three cases:

- A single step size yields circles representing lines of equal probability, Fig. 1 (left). This step size is a scalar and called *global* step size. It represents the standard deviation of the mutation.
- Step sizes, different in each coordinate direction of the parameter space, correspond to mutation ellipses which are parallel to the coordinate axes, Fig. 1 (middle). These step sizes can

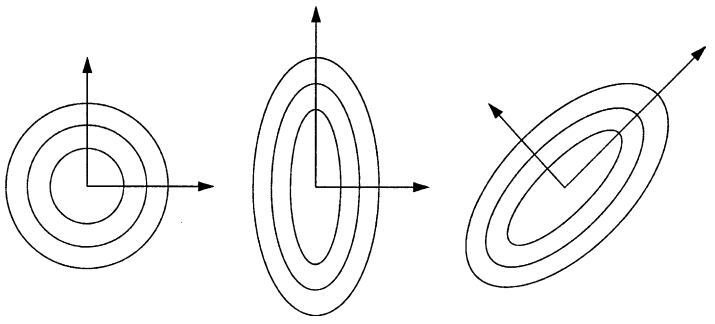

Fig. 1. Isoprobability contours in two dimensions for three probability densities used for the mutation step. Left: isotropic Gaussian density of $\boldsymbol{z}$. Middle: scaled probability density. Right: scaled and rotated probability density.

be summarized in an n-dimensional vector and they are referred to as *individual* step sizes. The standard deviation of the mutation is different in each coordinate axis.

- Correlated mutations, generated by a linear transformation of a $\mathcal{N}(\mathbf{0}, \boldsymbol{I})$ normally distributed random vector, give rise to arbitrarily oriented mutation ellipses, Fig. 1 (right). Step sizes can be presented by an $n \times n$ matrix, the so-called covariance matrix $\boldsymbol{C}$. The diagonal entries of $\boldsymbol{C}$ contain the variances of the mutation, and the off-diagonal entries are the covariances.

3.3. Covariance matrix adaptation

In the present study, we use an evolution strategy with adaptation of the covariance matrix. The covariance matrix adaptation evolution strategy (CMA-ES) approximates a mutation distribution which is properly adapted to the local topology of the objective function landscape. It performs a principal component analysis of the weighted mutation steps. The CMA-ES has been found to converge much faster than evolution strategies with only global and/or individual step size control for non-separable and badly scaled functions [8].

To mutate a parameter vector with a vector that is $\mathcal{N}(\mathbf{0}, \boldsymbol{C})$ distributed, we take a normally distributed vector $\boldsymbol{z} \sim \mathcal{N}(\mathbf{0}, \boldsymbol{I})$ and transform it linearly by a $n \times n$ matrix $\sqrt{\boldsymbol{C}}$. The vector $\sqrt{\boldsymbol{C}}\boldsymbol{z}$ is then $\mathcal{N}(\mathbf{0}, \boldsymbol{C})$ distributed. By construction, $\boldsymbol{C}$ is the covariance matrix of the mutation distribution. To control the overall variance, $\sqrt{\boldsymbol{C}}\boldsymbol{z}$ is multiplied by the global step size σ.

The mutation step in the (μ_I, λ)-CMA-ES reads then:

$$\boldsymbol{x}_k^{(g+1)} = \langle \boldsymbol{x} \rangle_\mu^{(g)} + \sigma^{(g)} \underbrace{\sqrt{\boldsymbol{C}^{(g)}}\boldsymbol{z}_k}_{\sim \mathcal{N}(\mathbf{0}, \boldsymbol{C}^{(g)})}, \quad k = 1, \ldots, \lambda. \tag{5}$$

$\langle \boldsymbol{x} \rangle_\mu^{(g)}$ is the intermediate recombination (average) of μ selected parameter vectors.

The adaptation mechanism can be distinguished in two parts: (i) the adaptation of the covariance matrix $\boldsymbol{C}^{(g+1)}$, and (ii) the adaptation of the global step size $\sigma^{(g+1)}$. This distinction is motivated as follows: The covariance matrix can be adapted only on a larger time scale as selection information for the adaptation of $(n^2 + n)/2$ matrix elements has to be collected before doing notable changes. On the other hand, the adaptation of the global step size, a scalar, requires less selection information, and thus it changes on a shorter time scale.

A detailed description of the CMA-ES including the two adaptation mechanisms can be found in [9,10]. We use strategy parameters as defined in [9].

4. Optimization results

4.1. Numerical method

The flow in the micromixer is governed by the incompressible Navier–Stokes equation

$$\frac{\mathrm{D}\mathbf{v}}{\mathrm{D}t} = -\nabla p + \frac{1}{Re}\nabla^2 \mathbf{v}, \quad \nabla \cdot \mathbf{v} = 0. \tag{6}$$

The mixing of two fluid streams of uniform and equal properties is governed by the convection–diffusion equation

$$\frac{\mathrm{D}c}{\mathrm{D}t} = \frac{1}{Pe}\nabla^2 c, \tag{7}$$

where c is the concentration, $Pe = U_m h/\kappa$ is the Peclet number, and κ is the molecular diffusivity. In the present study, we set $\kappa = 2 \times 10^{-9}$, and hence $Pe = 5 \times 10^8$.

The Navier–Stokes and convection–diffusion equations are discretized using a second order finite volume technique and solved on a Cartesian coordinate system using a standard computational fluid dynamics package [1]. The main flow channel contains 20×135 grid points in the span- and streamwise direction, respectively, while the secondary channels are discretized using 5×50 grid points each. The initial conditions involve a uniform concentration of zero and unity for the grid points below and above the symmetry line ($y = 0$). The mixing rate m is estimated from the local variance of the concentration field,

$$m = \overline{c^2} - \bar{c}^2 \tag{8}$$

and $\bar{c}$ denotes the mean (spatial) concentration in the region A (Fig. 2), extending between $x = 12h$ and $x = 13.5h$, located downstream of the third secondary channel. Note, $m = 0$ indicates perfect mixing and $m = 0.25$ zero mixing.

In a preliminary study, the mixing rate was furthermore estimated by observing the mixing of fluid markers (particles) continuously added at the inlet (at $x = 0$). Although this Lagrangian technique does not account for diffusion of mass, if was found to predict mixing rates similar to the computationally more efficient Eulerian approach (Eq. (7)).

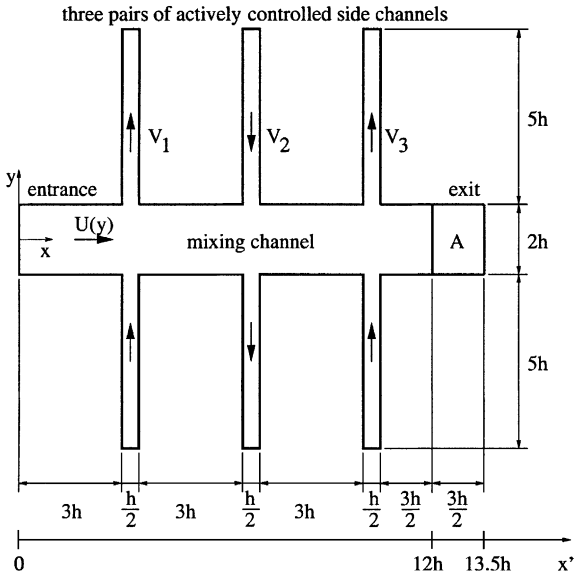

Fig. 2. Schematic of the flow configuration. Flow in the main channel is manipulated by controlling time-dependent flow from six secondary channels. The mixing rate is averaged in the region A.

4.2. Optimization parameters, function, and algorithm

We optimize the mixing rate for three types of actuation:

- $\boldsymbol{x} = (f_1, f_2, f_3)$ (three-frequency actuation),
- $\boldsymbol{x} = (f_1, f_2), f_3 = 0$ (two-frequency actuation), and
- $\boldsymbol{x} = (f_1), f_2 = f_3 = 0$ (one-frequency actuation).

The objective function is the mixing rate m as described above, averaged between the non-dimensional times $t = TU_m/h = 90$ and 135, a quasi-periodic time regime. The time $t = 135$ corresponds to 10 flow through times which is defined as

$$T_f = \frac{L}{U_m} = \frac{13.5h}{U_m} = 13.5. \tag{9}$$

The computational cost for one function evaluation, i.e. one flow simulation until time $t = 135$, is approximately 3 CPU hours on a Sun Sparc Ultra-2 processor.

The optimization algorithm is a CMA-ES [9] with a population that consists of $\mu = 2$ parents and $\lambda \in [8, 10]$ children. Using explicit message passing paradigms (MPI), the optimization is performed in parallel on a cluster of $\lambda/2$ Sun workstations. Due to the high computational cost, we perform only one optimization run for each type of actuation. Thus, our results are compared with theoretical arguments as described in Section 2.

4.3. Discussion

The initial and the optimized parameters and the mixing rates for the three different types of actuation (the three-, two-, and one-frequency actuation) are summarized in Table 1.

For the three-frequency actuation, we obtain the following mixing rates: With identical frequencies $\left(\frac{1}{2}, \frac{1}{2}, \frac{1}{2}\right)$, motivated by the first theoretical approximation, the mixing rate is 0.1596. The initial "rational" frequencies $\left(\frac{1}{2}, \frac{1}{3}, \frac{1}{4}\right)$ results in a mixing rate of 0.0345, and the theoretical or

Table 1
Initial and optimized frequencies for the three different types of actuation

		Number of actuated frequencies		
		3	2	1
Initial frequencies	f_1	0.25	0.50	0.50
	f_2	0.33	0.50	0
	f_3	0.50	0	0
Initial mixing rate	m	0.0345	0.1660	0.1825
Optimized frequencies	f_1	0.14	0.14	0.15
	f_2	0.32	0.32	0
	f_3	0.50	0	0
Optimized mixing rate	m	0.0213	0.0370	0.0600
Number of function evaluations		460	320	64

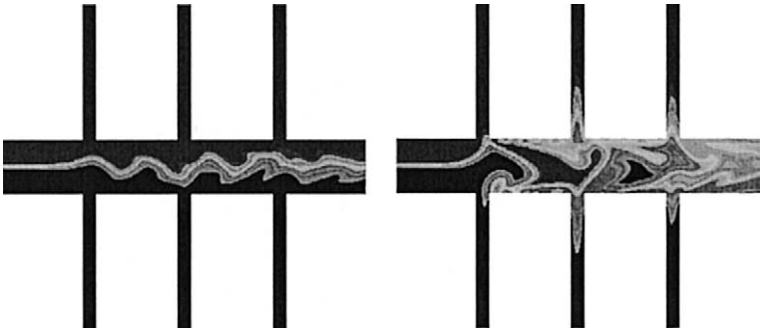

Fig. 3. Snapshots of the concentration field of the flow actuated by the frequencies in the three side-channel pairs $\boldsymbol{x} = (1/2, 1/2, 1/2)$ (left) obtained by theoretical arguments, and by the optimal frequencies $\boldsymbol{x} = (0.14, 0.32, 0.50)$ (right) obtained using evolutionary optimization.

"irrational" frequencies as proposed in Volpert et al. [19] $\left(\frac{1}{2\sqrt{5}}, \frac{1}{2\sqrt{2}}, \frac{1}{2}\right)$ in a value of 0.0285. The evolutionary optimization yields a mixing rate of 0.0213 with frequencies (0.14, 0.32, 0.50). Thus, the optimization reduces the mixing rate to 62% of the initial function value, and improves the theoretical mixing rate by 25%. The optimized parameters appear to be irrational numbers. However, due to the rather low precision of the optimized parameters, we cannot really argue that their ratio is rational or irrational. The optimized frequencies were obtained after 17 generations (170 function evaluations). We continued the optimization until 46 generations (460 function evaluations) to check the sensitivity of the found solution. During this phase, $17 < g < 46$, the mixing rate was found to differ by less than 2%. Thus, we consider the value converged. Fig. 3 shows two snapshots of the concentration field in the micromixer at time $t = 45$ for the identical and optimal frequencies, respectively. We observe that the mixing using optimized frequencies is indeed improved significantly compared with the identical frequencies.

For the two-frequency actuation, the optimized mixing rate of 0.0370 is reduced drastically to 22% of the initial mixing rate of 0.1660 for identical frequencies $\left(\frac{1}{2}, \frac{1}{2}, 0\right)$. For the actuation of two frequencies, we found that similar actuation frequencies, (0.265, 0.269, 0), result in low frequency oscillations of the flow, thus requiring longer sampling times than the selected $t = 135$. The oscillations resulted in inaccurately determined mixing rates, but consistently lower values for the mixing rate (0.0217). However, the recombination (averaging) feature of the CMA-ES managed to deal with this difficulty by averaging the actuation frequencies of the child parameter vectors. The similar frequencies appeared after 15 generations (120 function evaluations), causing a slowdown of the optimization process. The optimization converged after 29 generations with a variation less than 9% between $g = 29$ and $g = 40$ (232 and 320 function evaluations). From the function points computed during the optimization, we reconstructed the mixing rate landscape as a function of the actuation parameters. The landscape is visualized in Fig. 4.

The one-frequency actuation yields a mixing rate decreased to 33% of the initial mixing rate for $\left(\frac{1}{2}, 0, 0\right)$. The mixing rate between 6 and 8 generations (48 and 64 function evaluations) differs less than 1%. After 8 generations, the optimization is stopped. The optimal frequency of the first side channel appears to be independent of the number of actuated side channels and is $f_1 = 0.15$.

In the three optimizations, the first parameter attains values of about $f_1 \approx 0.14$–0.15, indicating that the optimization function is separable. The same phenomenon occurs for the second

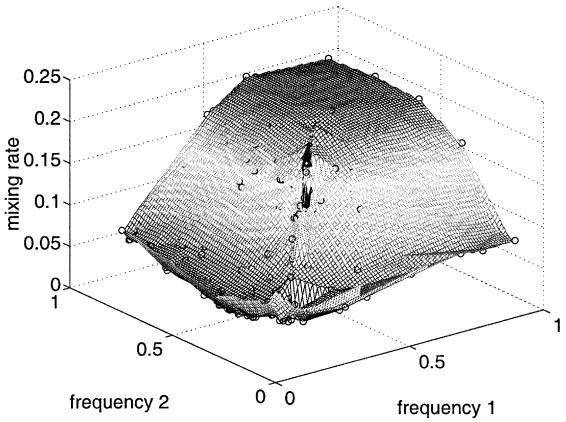

Fig. 4. Surface of the mixing rate as a function of the two actuation frequencies, constructed from points computed during the optimization (○).

frequency for the optimization of two and three frequencies where $f_2 = 0.32$. Thus, it appears that optimal frequencies are independent of the number of actuated side channels. This is quite surprising given that the mixing process is highly non-linear. If this result is generalizable to different geometrical micromixer configurations remains a subject of future research.

5. Conclusions

The results presented herein for the optimization of micromixing suggest that evolution strategies can be a valuable tool complementing physical understanding and theoretical prediction techniques. Due to the high computational cost associated with the evaluation of the cost function, we have not pursued alternative optimization strategies to allow comparison with the present approach. Other optimization strategies may converge to the optimum faster than the proposed evolution strategy. However, the robustness of the chosen evolution strategy with covariance matrix adaptation has enabled us to avoid getting trapped in local optima, present in this optimization problem.

For mixing configurations with two- and three-frequency actuation, the frequency ratios resulting from our evolutionary optimization resemble theoretical considerations. The optimization of the micromixer with one-, two-, and three-frequency actuation yields highly improved mixing rates compared with the best mixing rates suggested by theoretical arguments. Another rather surprising but interesting result is that optimal frequencies for increasing number of transverse channels are superposable despite the non-linear nature of the mixing process.

Future research includes studies in different mixer geometries, including three-dimensional effects.

References

[1] Star-CD User Manual. Computational Dynamics Ltd., London, 1997.
[2] Aref H. Stirring by chaotic advection. J Fluid Mech 1984;143:1–21.

[3] Branebjerg J, Fabius B, Gravesen P. Application of miniature analyzers from microfluidic components to mTAS. In: Proceedings of Micro Total Analysis System Conference, Twente, Netherlands, 1994. p. 141–51.
[4] Branebjerg J, Fabius B, Gravesen P. Fast mixing by lamination. In: Proceedings of the 9th Annual Workshop on MEMS, San Diego, CA, 1996. p. 441–6.
[5] Chiem N, Colyer C, Harrison DJ. Microfluidic systems for clinical diagnostics. In: International Conference on Solid State Sensors and Actuators, Chicago, IL, vol. 1. 1997. p. 183–6.
[6] D'Alessandro D, Dahleh M, Mezić I. Control of mixing in fluid flow: a maximum entropy approach. IEEE Trans Automatic Control 1999;44:1852–63.
[7] Evans J, Liepmann D, Pisano AP. Planar laminar mixer. In: 10th Annual Workshop of Micro Electro Mechanical System, Nagoya, Japan, 1997. p. 96–101.
[8] Hansen N. Verallgemeinerte individuelle Schrittweitenregelung in der Evolutionsstrategie. Eine Untersuchung zur entstochastisierten, koordinatensystemunabhängigen Adaptation der Mutationsverteilung. Berlin: Mensch und Buch Verlag; 1998. ISBN 3-933346-29-0.
[9] Hansen N, Ostermeier A. Convergence properties of evolution strategies with the derandomized covariance matrix adaptation: the $(\mu/\mu_I, \lambda)$-CMA-ES. In: Zimmermann H-J, editor. EUFIT'97, 5th Europ Congr on Intelligent Techniques and Soft Computing, Proceedings, Aachen, Germany. Verlag Mainz; 1997. p. 650–4.
[10] Hansen N, Ostermeier A. Completely derandomized self-adaptation in evolution strategies. Evol Comput 2001;9(2):159–95.
[11] Lee YK, Tabeling P, Shih C, Ho C-M. Characterization of a MEMS-fabricated mixing device. In: Proceedings of MEMS-Vol 2, Micro-electro-mechanical systems. Orlando, FL: ASME; 2000.
[12] Lichtenberg AJ, Lieberman MA. Regular and chaotic dynamics. New York: Springer-Verlag; 1992.
[13] Liu RH, Sharp KV, Olsen MG, Stremler MA, Santiago JG, Adrian RJ, et al. A passive micromixer three-dimensional serpentine microchannel. J MEMS 2000;9(2).
[14] Miyake R, Lammerink TSJ, Elwenspoek M, Fluitman JHJ. Micro mixer with fast diffusion. In: Proceedings of the IEEE MEMS Workshop, Fort Lauderale, FL, 1993. p. 248–53.
[15] Ottino JM. The kinematics of mixing: stretching, chaos and transport. Cambridge: Cambridge Univ Press; 1989.
[16] Rechenberg I. Evolutionsstrategie, Optimierung technischer Systeme nach Prinzipien der biologischen Evolution. Stuttgart: frommann-holzboog; 1973.
[17] Schwefel H-P. Evolution and optimum seeking. In: Sixth-generation computer technology series. New York: John Wiley & Sons Inc; 1995.
[18] Volpert M, Mezić I, Meinhart CD, Dahleh M. Modeling and analysis of mixing in an actively controlled micromixer. Unpublished report, University of Santa Barbara, CA, 2000.
[19] Volpert M, Mezić I, Meinhart CD, Dahleh M. Modeling and numerical analysis of mixing in an actively controlled micromixer. In: Proceedings of HEFAT2002, 1st International Conference on Heat Transfer, Fluid Mechanics, and Thermodynamics, Kruger Park, South Africa, 2001.
[20] Wiggins S. Introduction to applied nonlinear dynamical systems and chaos. New York: Springer-Verlag; 1990.
[21] Yi M, Bau HH. The kinematics of bend-induced stirring in micro-conduits. In: Proceedings of MEMS-Vol 2, MEMS. Orlando, FL: ASME; 2000.